

A Simple Class of Photorheological Fluids: Surfactant Solutions with Viscosity Tunable by Light

Aimee M. Ketner, Rakesh Kumar, Tanner S. Davies, Patrick W. Elder, and Srinivasa R. Raghavan*

Contribution from the Department of Chemical and Biomolecular Engineering, University of Maryland, College Park, Maryland 20742-2111

Received July 15, 2006; Revised Manuscript Received November 5, 2006; E-mail: sraghava@eng.umd.edu

Abstract: Photorheological (PR) fluids, i.e., those with light-tunable rheological properties, may be useful in a variety of applications, such as in sensors and microfluidic devices. Currently, the need to synthesize complex photosensitive molecules hampers the applicability of these fluids. Here, we report a simple class of PR fluids that require no special synthesis and can be easily replicated in any lab from inexpensive chemicals. The fluids consist of the cationic surfactant, cetyl trimethylammonium bromide (CTAB), and the photoresponsive organic derivative, *trans-ortho*-methoxycinnamic acid (OMCA). Aqueous mixtures of CTAB and OMCA in basic solution self-assemble into long, wormlike micelles. Upon irradiation by UV light (<400 nm), OMCA undergoes a photoisomerization from its *trans* to its *cis* form, which alters the molecular packing at the micellar interface. The result is to transform the long micelles into much shorter entities and, in turn, the solution viscosity decreases by *more than 4 orders of magnitude*. Small-angle neutron scattering (SANS) is used to confirm the dramatic reduction in micellar length. The extent of viscosity reduction in these PR fluids can be tuned based on the composition of the mixture as well as the duration of the irradiation.

1. Introduction

Recently, there has been much interest in creating fluids whose rheological properties (such as viscosity) are tunable by light.^{1–3} Such fluids could be termed *photorheological* (PR) fluids,⁴ and could offer a third paradigm for rheology modulation, following in the path of existing electrorheological (ER) fluids⁵ that are sensitive to electric fields and magnetorheological (MR) fluids that respond to magnetic fields.⁶ ER and MR fluids have been around for more than 50 years, and their ability to switch rheological states has formed the basis for technologies such as dampers, clutches, and valves.⁶ However, these fluids are typically two-phase systems that tend to aggregate or settle with time. PR fluids, on the other hand, promise to be true, single-phase solutions, structured at the nanoscale. Also, an advantage of light over electric or magnetic fields is that light can be directed at a precise spatial location; this becomes especially valuable in microscale or nanoscale applications. Accordingly, PR fluids could be an enabling technology for microfluidic or MEMS devices and sensors.

Despite their obvious potential, PR fluids are not used widely at the moment, in either scientific labs or commercial applications. The chief reason is that current PR fluid formulations

rely on complicated photoresponsive molecules, such as, for example, a photoresponsive surfactant or polymer bearing an azobenzene moiety.^{2,7–9} Several groups have demonstrated reversible viscosity modulation using such photosensitive moieties. The principle in each case has been to control the reversible self-assembly of the photosensitive surfactant and/or polymer between a nanostructure that yields a high viscosity (e.g., a transient network) and one that corresponds to weaker association and thereby a low viscosity. However, the difficulty in synthesizing these types of molecules has meant that the corresponding PR fluids remain accessible only to a few select research groups. There is thus a need for new PR fluids that could be readily prepared anywhere from simple, existing molecules.

In this paper, we report a new class of PR fluids that are based entirely on simple, inexpensive chemicals available to any lab. The fluids are composed of the cationic surfactant, cetyl trimethylammonium bromide (CTAB), together with a photo-sensitive organic acid or salt. While we have studied a number of such additives, we focus specifically on *trans-ortho*-methoxycinnamic acid (OMCA) in this paper. We show that CTAB/OMCA mixtures form wormlike micelles^{10–13} in aqueous solution and that, upon irradiation by UV light (<400 nm), the

- (1) Paulusse, J. M. J.; Sijbesma, R. P. *Angew. Chem., Int. Ed.* **2006**, *45*, 2334–2337.
- (2) Eastoe, J.; Vesperinas, A. *Soft Matter* **2005**, *1*, 338–347.
- (3) Tomatsu, I.; Hashidzume, A.; Harada, A. *Macromolecules* **2005**, *38*, 5223–5227.
- (4) Wolff, T.; Emming, C. S.; Suck, T. A.; Von Bunau, G. *J. Phys. Chem.* **1989**, *93*, 4894–4898.
- (5) Hao, T. *Adv. Mater.* **2001**, *13*, 1847–1857.
- (6) Rankin, P. J.; Ginder, J. M.; Klingenberg, D. J. *Curr. Opin. Colloid Interface Sci.* **1998**, *3*, 373–381.

- (7) Lee, C. T.; Smith, K. A.; Hatton, T. A. *Macromolecules* **2004**, *37*, 5397–5405.
- (8) Sakai, H.; Orihara, Y.; Kodashima, H.; Matsumura, A.; Ohkubo, T.; Tsuchiya, K.; Abe, M. *J. Am. Chem. Soc.* **2005**, *127*, 13454–13455.
- (9) Pouliquen, G.; Tribet, C. *Macromolecules* **2006**, *39*, 373–383.
- (10) Cates, M. E.; Candau, S. J. *J. Phys.: Condens. Matter* **1990**, *2*, 6869–6892.
- (11) Berret, J. F. In *Molecular Gels*; Weiss, R. G., Terech, P., Eds.; Springer: Dordrecht, 2005; pp 235–275.
- (12) Raghavan, S. R.; Kaler, E. W. *Langmuir* **2001**, *17*, 300–306.

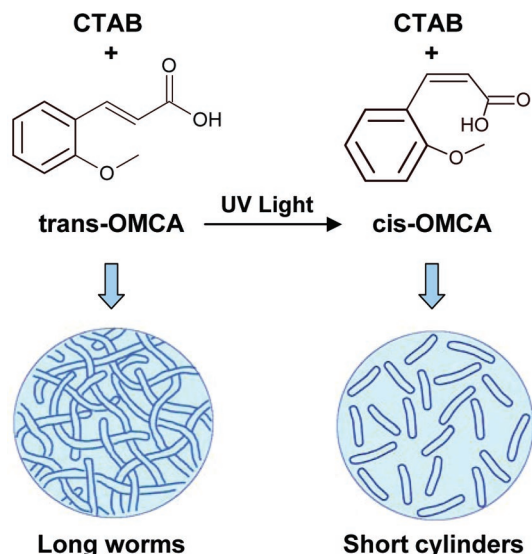


Figure 1. Schematic behavior of photoresponsive (PR) fluids consisting of CTAB and OMCA. When OMCA is in its *trans* form, its mixture with CTAB gives rise to long, entangled wormlike micelles. Upon UV irradiation, *trans*-OMCA gets photoisomerized to *cis*-OMCA, and the corresponding change in molecular geometry causes a drastic reduction in micellar length.

viscosity of these solutions can be made to drop by more than 4 orders of magnitude. The basis for this viscosity change is the *trans* to *cis* photoisomerization of the double bond in OMCA (Figure 1). The resultant change in the geometry of OMCA alters the molecular packing of the CTAB/OMCA complex, leading to a drastic reduction in the length of the wormlike micelles (Figure 1). In turn, the sample is transformed from a highly viscoelastic, gel-like fluid to a thin, runny fluid with a viscosity close to that of water. Confirmation of the above microstructural hypothesis is provided by data from small-angle neutron scattering (SANS).

Micellar systems based on photosensitive additives have been investigated for a long time, following the pioneering work of Wolff and co-workers (indeed, to our knowledge, it was Wolff who coined the term “photorheological fluid”).^{4,14–16} Past studies have mainly focused on anthracene and stilbene derivatives added to cationic surfactants. However, the viscosity change induced by light in these samples was rather modest (\sim a factor of 2–10).^{4,16} Thus, the principal result here is that much larger viscosity changes (factors of 1000 to 10,000) can be achieved in CTAB/OMCA mixtures. We should also note that the photosensitivity of OMCA is analogous to that of coumaric acid, which in turn is a key component of the “photoactive yellow protein”.¹⁷ Although, in principle, photoisomerizations are reversible, the *trans*–*cis* isomerization of OMCA is not easily reversed, and we will discuss the reasons for this later in the paper. This means that CTAB/OMCA mixtures can only provide a one-way viscosity switch. Nevertheless, the simplicity and ease of preparation of these mixtures should make them attractive for use in some microfluidic or sensor applications. Also, the underlying principle behind this work, namely, the ability to fine-tune micellar assembly by exploiting molecular

geometry, should be applicable to similar organic additives where the photoisomerization can indeed be reversed by irradiation at a different light wavelength. We hope that this work will stimulate studies into new types of PR fluids as well as applications for these fluids in microscale devices.

2. Experimental Section

Materials. CTAB was purchased from Sigma-Aldrich and was greater than 98% in purity. OMCA in its *trans* form was purchased from Acros Chemicals, while the *cis* form was purchased from TCI America, and each compound was greater than 98% in purity. All chemicals were used as received. Ultrapure deionized water from a Millipore water purification system was used in preparing samples for rheological characterization, while D₂O (99.95% deuterated, from Cambridge Isotopes) was used for the SANS studies. Solutions containing OMCA were prepared with a slight excess of base (NaOH), and CTAB was then added to these solutions to reach the final composition. Samples were stirred continuously under mild heat until they became homogeneous. The solutions were then left to equilibrate overnight at room temperature before any experiments were conducted. The pH in the samples was between 9 and 11.

Sample Response before and after UV Irradiation. CTAB/OMCA samples were irradiated with UV light from a Oriel 200 W mercury arc lamp. A dichroic beam turner with a mirror reflectance range of 280 to 400 nm was used to access the UV range of the emitted light. Samples (5 mL) were placed in a Petri dish with a quartz cover, and irradiation was done for a specific duration under stirring. Due to the nature of the OMCA spectra, irradiated samples did not undergo any changes when stored under ambient conditions, which made it easy to conduct subsequent tests using appropriate techniques such as UV–vis spectroscopy, HPLC, rheology, and SANS. UV–vis spectroscopy before and after irradiation were carried out using a Varian Cary 50 spectrophotometer.

HPLC Studies. The irradiated solutions were analyzed using HPLC (Waters Spherisorb 5 μ m ODS2, 4.6 mm \times 250 mm C18 column). A flow rate of 0.8 mL/min was used, and the eluting solvent was 15% ethanol and 85% water. The solution components were detected using UV absorption (Dynamax absorbance detector model UV-D II) at 225 and 254 nm. These parameters were based on those of a study of similar molecules by Imae et al.¹⁸ HPLC chromatograms of solutions before and after irradiation are provided as part of the Supporting Information.

Rheological Studies. Steady and dynamic rheological experiments were performed on an AR2000 stress controlled rheometer (TA Instruments, Newark, DE). Samples were run at 25 $^{\circ}$ C on a cone-and-plate geometry (40-mm diameter, 2 $^{\circ}$ cone angle) or a couette geometry (rotor of radius 14 mm and height 42 mm, and cup of radius 15 mm). Dynamic frequency spectra were obtained in the linear viscoelastic regime of each sample as determined by dynamic stress-sweep experiments.

Solubility Studies. The solubility of OMCA isomers in water at 25 $^{\circ}$ C was determined as follows, much like in an earlier study.¹³ An excess of the organic derivative was added to deionized water, and the solution was stirred under mild heat for 1 day, followed by equilibration at room temperature for two more days. A sample of this solution in a 1 mm cuvette was placed in the holder of the UV–vis spectrophotometer, maintained at 25 $^{\circ}$ C. The sample was left undisturbed for 1 h to allow any undissolved material to settle to the bottom of the cuvette. The absorbance was then measured and converted to a concentration value using the absorptivity determined from a calibration curve. The same procedure was repeated for each of the OMCA isomers.

Small Angle Neutron Scattering (SANS). SANS measurements were made on the NG-7 (30 m) beamline at NIST in Gaithersburg, MD. Neutrons with a wavelength of 6 \AA were selected. Two sample–

- (13) Davies, T. S.; Ketner, A. M.; Raghavan, S. R. *J. Am. Chem. Soc.* **2006**, *128*, 6669–6675.
 (14) Muller, N.; Wolff, T.; von Bunau, G. *J. Photochem.* **1984**, *24*, 37–43.
 (15) Wolff, T.; Klausner, B. *Adv. Colloid Interface Sci.* **1995**, *59*, 31–94.
 (16) Yu, X. L.; Wolff, T. *Langmuir* **2003**, *19*, 9672–9679.
 (17) Kort, R.; Vonk, H.; Xu, X.; Hoff, W. D.; Crielgaard, W.; Hellingwerf, K. J. *FEBS Lett.* **1996**, *382*, 73–78.

- (18) Imae, T.; Tsubota, T.; Okamura, H.; Mori, O.; Takagi, K.; Itoh, M.; Sawaki, Y. *J. Phys. Chem.* **1995**, *99*, 6046–6053.

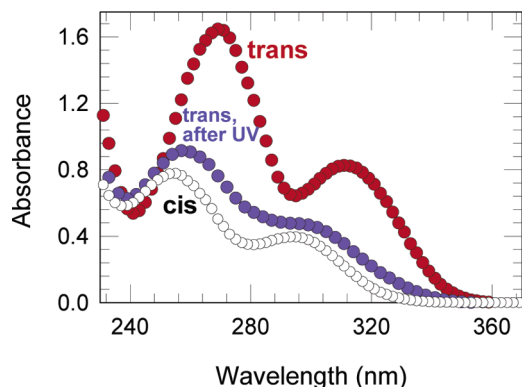


Figure 2. UV-vis spectra of *trans*-OMCA before irradiation, *trans*-OMCA after UV irradiation, and *cis*-OMCA. Each sample is an aqueous solution containing 1 mM of the corresponding additive. The drop in absorbance and blue shift in the *trans*-OMCA curve after UV irradiation indicate that the molecule has been photoisomerized to its *cis* form.

detector distances of 1.33 and 13.2 m were used to probe a wide range of wave vectors from 0.004 to 0.4 Å⁻¹. Samples were studied in 2 mm quartz cells at 25 °C. The scattering spectra were corrected and placed on an absolute scale using calibration standards provided by NIST. The data are shown for the radially averaged intensity I versus the wave vector $q = (4\pi/\lambda) \sin(\theta/2)$, where λ is the wavelength of incident neutrons and θ is the scattering angle.

SANS Modeling. For dilute solutions of noninteracting scatterers, the SANS intensity $I(q)$ can be modeled purely in terms of the form factor $P(q)$ of the scatterers (i.e., the structure factor $S(q) \rightarrow 1$ in such cases). Here, we consider form factor models for two different micellar shapes: ellipsoids and rigid cylinders.¹⁹ In the expressions below, $(\Delta\rho)$ is the difference in scattering length density between the micelles and the solvent, so that $(\Delta\rho)^2$ is the scattering contrast. The models were implemented using software modules supplied by NIST.

A. Ellipsoids. The form factor $P(q)$ for ellipsoids of revolution with minor and major axes R_a and R_b is given by¹⁹

$$P(q) = (\Delta\rho)^2 \left(\frac{4}{3} \pi R_a R_b^2 \right)^2 \int_0^1 \left[3 \frac{(\sin z - z \cos z)}{z^3} \right]^2 d\mu \quad (1)$$

where $z = q \sqrt{\mu^2 R_b^2 + R_a^2 (1 - \mu^2)}$. Here μ is the cosine of the angle between the scattering vector q and the symmetry axis of the ellipsoid.

B. Rigid Cylinders. The form factor $P(q)$ for rigid cylindrical rods of radius R and length L is given by¹⁹

$$P(q) = (\Delta\rho)^2 (\pi R^2 L)^2 \int_0^{\pi/2} [F(q, \alpha)]^2 \sin \alpha d\alpha \quad (2)$$

where

$$F(q, \alpha) = \frac{J_1(qR \sin \alpha)}{(qR \sin \alpha)} \cdot \frac{\sin(qL \cos \alpha/2)}{(qL \cos \alpha/2)} \quad (3)$$

Here α is the angle between the cylinder axis and the scattering vector q , and $J_1(x)$ is the first-order Bessel function of the first kind.

3. Results and Discussion

We first present UV-vis spectra for *trans* and *cis*-OMCA in Figure 2. These experiments were done with aqueous solutions containing 1 mM of the corresponding derivatives along with a slight excess of base. Figure 2 shows that the *trans* form has absorbance peaks at 270 and 312 nm, whereas the peaks for the *cis* form occur at 254 and 293 nm. Note that the *trans* form has much higher absorbances than the *cis* form. Thus, irradiation

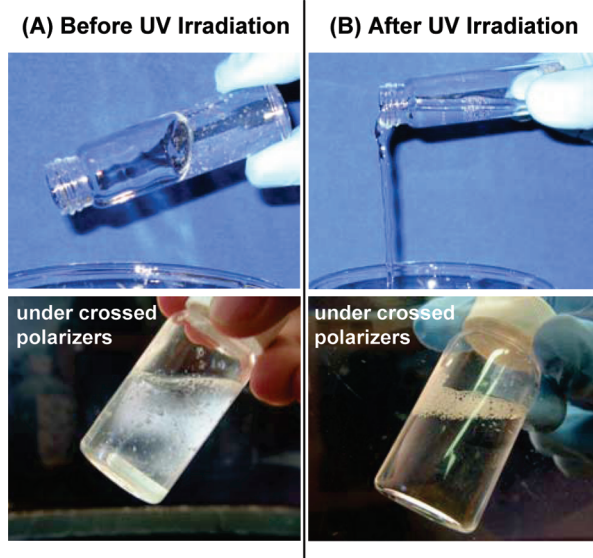


Figure 3. Photographs of a 60 mM CTAB + 50 mM OMCA sample (A) before and (B) after UV irradiation. (A) Initially, OMCA is in its *trans* form, and the sample is highly viscoelastic due to the presence of long worms. Consequently, the sample does not flow even when the vial is tilted (top) and retains bubbles for a long time (bottom). Moreover, the sample shows flow-birefringence; i.e., when viewed under crossed polarizers, streaks of light appear when the sample vial is lightly shaken (bottom). (B) Upon UV irradiation, OMCA is isomerized to its *cis* form, leading to much shorter micelles. In turn, the sample viscosity is significantly reduced, as shown by its rapid pourability (top) and by the rapid rise of bubbles to the liquid surface (bottom). Also, the flow-birefringence is no longer observed (bottom).

of the *trans* derivative with UV light will cause the molecule to absorb light, and this, in turn, can trigger a photoisomerization to its *cis* state, very similar to what occurs for other cinnamic acid derivatives. To test this, we irradiated the *trans*-OMCA solution with UV light and recorded UV-vis spectra after irradiation. As shown in Figure 2, UV irradiation causes a blue shift in the UV spectrum of *trans*-OMCA, with the peaks shifting to 257 and 300 nm (the peak heights are also significantly reduced). This blue shift is indicative of a *trans* to *cis* photoisomerization. Importantly, the shift in the spectrum can be effected by just 1 min of UV irradiation, and no further changes in the spectrum occur with longer irradiation times. The irradiated sample thus corresponds to a photostationary equilibrium of mostly *cis* (ca. 83%) molecules.

We now consider the effects of UV irradiation on mixtures of OMCA with the cationic surfactant, CTAB. Henceforth, the abbreviation OMCA will be used to refer to its *trans* form, which is the common, commercially available isomer. (On the other hand, *cis*-OMCA will be specifically denoted as such.) Incidentally, the presence of CTAB has no effect on the UV spectra of OMCA and thereby on the UV-induced *trans* to *cis* photoisomerization. Our initial studies with CTAB/OMCA mixtures showed that these could form highly viscous and viscoelastic solutions. For example, Figure 3 shows photographs of a sample containing 60 mM CTAB and 50 mM OMCA. This sample is viscous enough that it does not flow readily out of a tilted vial (Figure 3A). Also, when bubbles are introduced by shaking the vial, they remain trapped in the fluid for long periods of time. The sample also shows flow-birefringence; i.e., when viewed under crossed polarizers, streaks of light appear upon gently shaking or tapping the vial (Figure 3A).¹¹ Taken together,

(19) Pedersen, J. S. *Adv. Colloid Interface Sci.* **1997**, 70, 171–210.

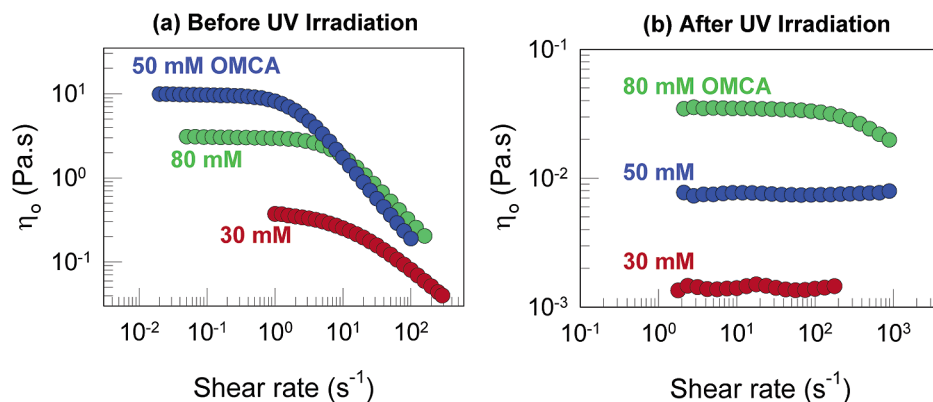


Figure 4. Viscosity vs shear rate plots for three CTAB/OMCA mixtures (a) before and (b) after UV irradiation for 30 min. The samples each contain 60 mM CTAB, and their OMCA concentrations are indicated on the plots. All samples show a shear-thinning response before irradiation, whereas, after irradiation, the samples are mostly Newtonian with much lower viscosities.

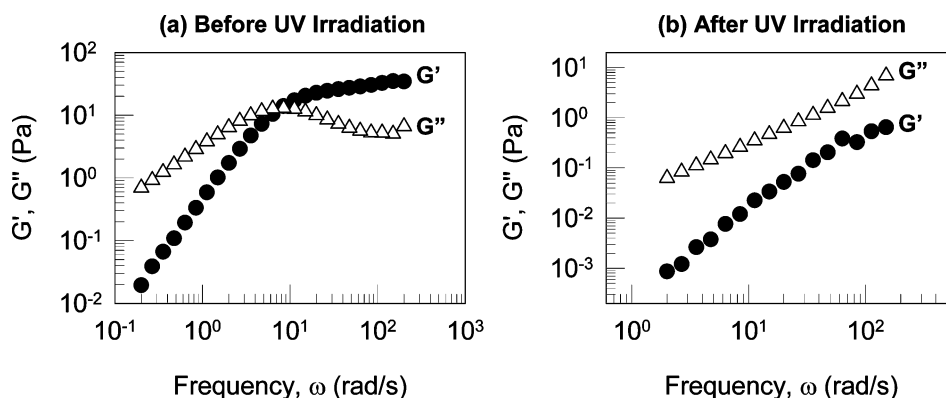


Figure 5. Dynamic rheology of a 60 mM CTAB + 80 mM OMCA sample (a) before and (b) after UV irradiation for 30 min. Before irradiation, the sample shows a viscoelastic response, whereas, after irradiation, its response is predominantly viscous.

the viscoelasticity and flow-birefringence suggest the presence of wormlike micelles, i.e., long, flexible, cylindrical chains in the CTAB/OMCA sample.^{11,13} On the other hand, CTAB/*cis*-OMCA mixtures are visually quite different. Those samples are low-viscosity, watery solutions that do not show any flow-birefringence (viscosity data for these mixtures will be presented later in Figure 7).

Based on the different rheological responses induced by the *trans* and *cis* forms of OMCA in CTAB mixtures, we were interested in examining the effects of light irradiation on sample rheology. Accordingly, we irradiated the 60 mM CTAB + 50 mM OMCA with UV light for 30 min. Figure 3B presents visual evidence for the effects induced by UV irradiation on the sample rheology. The photographs show that the sample has been converted to a thin, runny fluid that can be easily poured out of the vial and in which bubbles rapidly rise to the surface. Moreover, the irradiated sample does not show flow-birefringence. Thus, Figure 3 demonstrates a dramatic light-induced rheological transition in the CTAB/OMCA sample. Based on the spectra in Figure 2, the rheological change is clearly a result of the *trans* to *cis* photoisomerization of OMCA. We will show that this change in molecular geometry causes a dramatic reduction in micellar length, which explains the drop in viscosity.

We now present rheological data on selected CTAB/OMCA samples to quantify the light-induced rheological changes. Note that, following irradiation, CTAB/OMCA samples remain unaltered when stored under ambient conditions (exposure to

visible light has no effect because OMCA has a negligible absorbance in the visible range of the spectrum). Thus, irradiated samples could be tested subsequently on the rheometer. Figure 4 shows steady-shear rheological data (viscosity vs shear rate) for three samples, each containing 60 mM CTAB, with OMCA concentrations of 30, 50, and 80 mM, respectively. Before irradiation (Figure 4a), all three samples show shear-thinning behavior, with a plateau in the viscosity at low shear rates, followed by a decrease in viscosity at higher shear rates. The zero-shear viscosity η_0 is highest for the 50 mM OMCA sample, with a value of about 10 Pa·s (i.e., about 10,000 times the viscosity of water). With further increases in OMCA content, there is a drop in η_0 (this is further discussed under Figure 7), and the 80 mM OMCA sample has an η_0 value of about 2 Pa·s. Figure 4b shows the rheology of the same three samples after UV irradiation for 30 min. The irradiated samples show negligible shear rate-dependence of their viscosities; i.e., their behavior is mostly Newtonian (only the 80 mM OMCA sample shows slight shear-thinning). Moreover, the viscosities are much lower compared to Figure 4a, with each sample showing a drop in η_0 by several orders of magnitude due to UV irradiation. The measurements thus confirm the visual observations reported in Figure 3.

In addition to steady-shear rheology, it is useful to examine the rheological response under dynamic or oscillatory shear, which is a more sensitive probe of the nanostructure in complex fluids. Figure 5 shows dynamic rheological data on a sample containing 60 mM CTAB and 80 mM OMCA. The data are

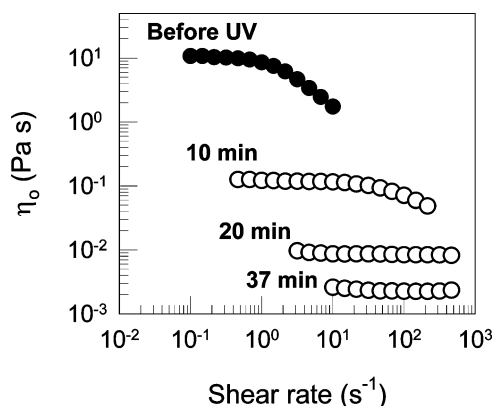


Figure 6. Steady-shear rheology of a 60 mM CTAB + 50 mM OMCA sample before irradiation and after UV irradiation for various periods of time (as indicated on the plot). The sample is observed to switch from a highly viscous, shear-thinning fluid to a low-viscosity, Newtonian fluid with progressive irradiation.

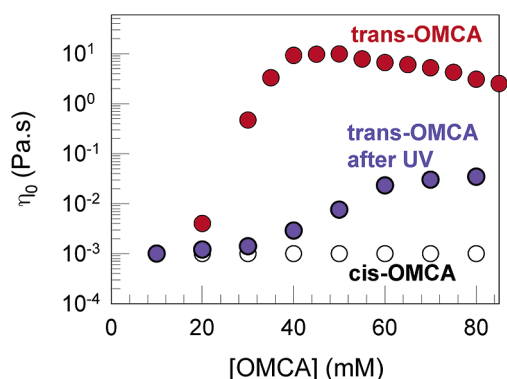


Figure 7. Zero-shear viscosity η_0 of 60 mM CTAB + OMCA mixtures as a function of the OMCA content. Data are shown for samples containing *trans*-OMCA, for *cis*-OMCA, and for *trans*-OMCA samples after 30 min of UV irradiation. A significant light-induced drop in viscosity is observed for the *trans*-OMCA samples.

presented as plots of the elastic modulus G' and viscous modulus G'' as functions of the angular frequency ω . Before irradiation (Figure 5a), the sample shows a typical viscoelastic response; i.e., the behavior is elastic ($G' > G''$, plateau in G' at high frequencies or short time scales, while it is viscous ($G'' > G'$, both moduli are strong functions of frequency) at low frequencies or long time scales. On the other hand, after irradiation with UV light for 30 min (Figure 5b), the sample exhibits a purely viscous response over the entire range of frequencies. Thus, dynamic rheology confirms a light-induced transition from a viscoelastic fluid to a thin, viscous one, again consistent with the photographs in Figure 3.

We have thus shown that appreciable rheological changes can be induced in CTAB/OMCA samples by UV irradiation. Next, we discuss the evolution of sample rheology as a function of irradiation time. Figure 6 shows viscosity vs shear rate plots for a 60 mM CTAB + 50 mM OMCA sample after various periods of UV irradiation. Before irradiation, the sample is highly viscous and strongly shear-thinning. After 10 min of irradiation, the zero-shear viscosity is reduced by about 2 orders of magnitude and the extent of shear-thinning is also reduced. After 20 min, the viscosity is further reduced and the sample behaves like a Newtonian fluid over the shear rates investigated. Finally, after 37 min, the viscosity drops to that of the solvent, i.e., water. No further changes in viscosity occur with longer

irradiation. The data show that the viscosity drop can be controlled through the irradiation time. It is worth pointing out here that the rate of viscosity reduction is determined primarily by the rate of absorption of UV light by the sample, which in turn depends on the intensity of the UV lamp, the sample volume used, and the experimental geometry (path length). Once light is absorbed by the OMCA molecules, they will photoisomerize on a time scale of milliseconds. In the above experiments, we did not attempt to optimize the transition speed, but it is easy to achieve faster viscosity transitions with CTAB/OMCA fluids. Indeed, preliminary experiments with smaller sample volumes show that a significant viscosity drop can be achieved within a few seconds.

The viscosity drop upon UV irradiation can also be controlled via the sample composition itself. Figure 7 shows the zero-shear viscosity η_0 of 60 mM CTAB solutions as a function of either *trans*-OMCA or *cis*-OMCA concentration. For the *trans*-OMCA samples, data are also shown after 30 min of UV irradiation. Note that the viscosities of CTAB/*cis*-OMCA solutions are very low and approximately identical to that of water. On the other hand, the viscosities induced by *trans*-OMCA are much higher and reach a peak around 50 mM of the additive (such a viscosity peak vs additive concentration is often seen for wormlike micelles^{11,12} and is believed to signify a transition from linear to branched worms). Upon UV irradiation of the *trans*-OMCA samples, the viscosities drop in all cases, with the extent of the drop being highest (ca. 10,000-fold) near the peak. It should be noted that, for all samples, irradiation for longer times will cause the viscosity to drop further until the photoisomerization is complete. At this stage, the viscosity will drop to that of the *cis*-OMCA samples, i.e., to a waterlike viscosity.

The above rheological and visual observations on CTAB/OMCA samples indicate a transition from long, wormlike micelles to much shorter micelles upon UV irradiation. To recap, before irradiation, the samples are flow-birefringent, they are viscoelastic under dynamic rheology, and shear-thinning in steady rheology. All these phenomena are associated with wormlike micelles: the flow birefringence arises because the worms tend to align along the flow direction when sheared, the viscoelastic behavior is due to the entanglement of the worms into a transient network, and the shear-thinning is caused by a disruption of this network due to shear.^{11,13} The absence of these phenomena in the irradiated sample suggests that the micelles have been reduced to much shorter (nonentangled) structures. In order to independently verify such a reduction in micellar size, we turn to a second technique, namely SANS.

Samples for SANS were made in D₂O to achieve the required contrast between the micellar structures and solvent. We verified that CTAB/OMCA samples in D₂O were rheologically identical to those made in H₂O. SANS data can be readily interpreted in terms of micelle size and shape only when intermicellar interactions (structure factor contributions) are minimized, i.e., when electrostatic interactions are screened and the micelle volume fraction is low. We therefore studied equimolar CTAB/OMCA samples at relatively low concentrations. SANS spectra (I vs q) are shown in Figure 8 for three samples with CTAB/OMCA concentrations of 30/30, 20/20, and 5/5 mM, respectively. In each case, data are shown before and after UV irradiation for 30 min. We note that, for all samples, irradiation

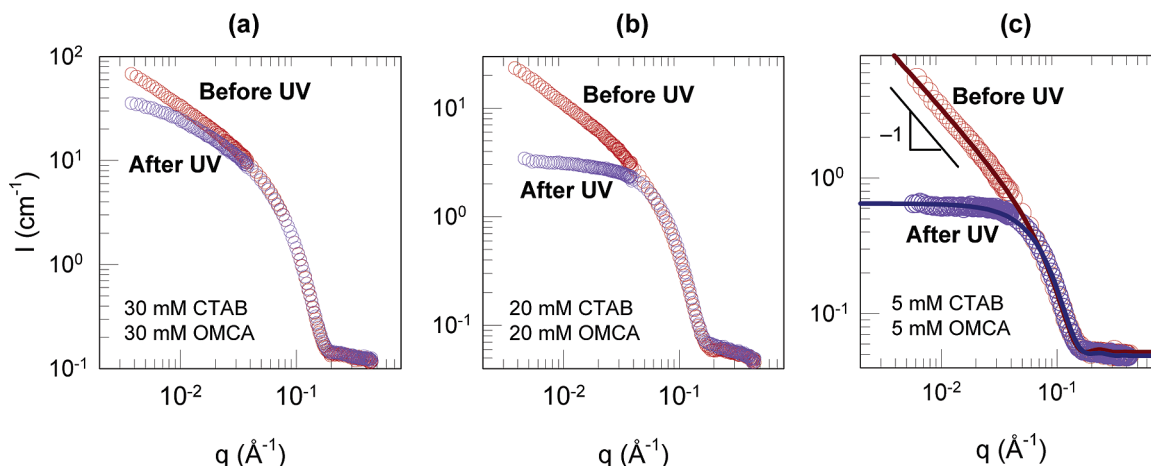


Figure 8. SANS scattering spectra from three CTAB/OMCA mixtures before and after 30 min of UV irradiation. The lines through the data for the 5/5 CTAB/OMCA sample are model fits to cylindrical micelles (before irradiation) and ellipsoidal micelles (after irradiation).

causes a significant drop in the scattered intensity at low q . The drop in intensity is a direct, qualitative indication of a decrease in micelle size, which is consistent with our expectation.

To obtain a more quantitative measure of micellar sizes, we model the SANS data from the 5/5 sample. For this sample (Figure 8c), a large decrease in intensity is seen upon UV irradiation, presumably because the micelle sizes fall within the window probed by SANS. Prior to irradiation, the intensity asymptotes at low q to a slope of about -1 , which is indicative of long, cylindrical structures.¹⁹ We therefore model the micelles as rigid cylinders (eqs 2, 3), and the fit is shown as a solid line through the data. From the fit, the micellar radius is obtained to be about 22 Å, while their length is ca. 3000 Å. The same sample after irradiation shows a plateau in SANS intensity at low q , which suggests the presence of smaller and more globular structures. Accordingly, we model the micelles in this case as ellipsoids of revolution (eq 1), and the corresponding fit is again shown as a solid curve through the data. A good fit is obtained for prolate ellipsoids with radii of 22 and 40 Å, respectively, for their major and minor axes. Thus, as expected, there is a dramatic reduction in the largest dimension of the micelles (a factor of about 100) due to UV irradiation.

The SANS data thus confirm that the light-induced viscosity reduction in CTAB/OMCA mixtures is due to a decrease in micelle size. The micellar size reduction, in turn, is evidently caused by the photoisomerization of OMCA from *trans* to *cis*, as indicated by the UV–vis spectra (Figure 2). Note that there is negligible evidence for other light-induced effects such as photodimerization in our samples (the latter has been shown to occur in certain mixtures of cinnamic acid and zwitterionic surfactants¹⁸). Indeed, HPLC studies on our solutions (see Supporting Information) confirm that photoisomerization of OMCA is the dominant light-induced effect. This hypothesis is consistent with the results of Figure 7, which show that *trans*- and *cis*-OMCA differ greatly in their ability to induce growth of CTAB micelles.

The question then is *why* are *trans*- and *cis*-OMCA so different? Can we rationalize these differences based on what we know about wormlike micelles and their self-assembly? We believe that there are two related factors to consider in this regard: (i) the geometry of the two OMCA isomers and (ii) their hydrophobicities. Both these factors will influence the association of OMCA with CTAB micelles. In turn, the

association of OMCA will reduce the micellar surface charge, thus decreasing the effective area of the charged headgroups and, thereby, facilitating the growth of long, cylindrical micelles. In other words, the key requirement for micellar growth is the association (adsorption) of OMCA counterions at the micellar interface.¹¹ Much like other aromatic counterions, OMCA is expected to adsorb in such a way that the hydrophobic aromatic ring is embedded in the hydrophobic interior of the micelle while the carboxylate anion is located next to the cationic headgroups at the interface.^{13,20} Also, the extra methyl group on OMCA must be preferably oriented toward the micelle interior as well. Such an orientation appears to be achievable for *trans*-OMCA but more difficult for *cis*-OMCA (Figure 1). In the case of *cis*-OMCA, the methyl and carboxylate moieties are brought into close proximity such that it will be difficult for the former to orient inward and the latter outward relative to the micellar interface. In short, geometric arguments suggest that *trans*-OMCA will strongly associate with CTAB micelles, whereas *cis*-OMCA will associate weakly.

A second related argument concerns the relative hydrophobicities of the two isomers: specifically, we believe that *trans*-OMCA is more hydrophobic than *cis*-OMCA. A greater hydrophobicity of the *trans* isomer has been noted for a variety of compounds, including olefinic and azobenzene derivatives. For example, in azobenzene-based surfactants, the greater hydrophobicity of the *trans* form gives it a lower critical micelle concentration or CMC.^{7,8} This difference in hydrophobicity has been attributed to the lower net dipole moment of the *trans* compared to the *cis* isomer: i.e., the dipoles add up in the *cis*, while they tend to cancel each other in the *trans* (equivalently, there is greater charge delocalization in the *cis* form).^{7,8} Moreover, our own studies further confirm the differences in hydrophobicity. In the absence of base, we find that *trans*- and *cis*-OMCA have limited solubility in deionized water. But while the solubility of *cis*-OMCA is measured to be 8.6 mM, the solubility of *trans*-OMCA is just 0.26 mM, i.e., more than a factor of 30 less. Accordingly, our solubility measurements confirm that *trans*-OMCA is much more hydrophobic than *cis*-OMCA, which suggests that the former will also remain associated with micelles to a much greater extent. Indeed, a lower solubility in water has been correlated with a greater

(20) Hassan, P. A.; Raghavan, S. R.; Kaler, E. W. *Langmuir* **2002**, *18*, 2543–2548.

association with micelles previously.¹³ All in all, the hydrophobicity arguments support the geometric reasoning advanced above.

Our arguments ultimately lead to the following mechanism to explain our results: when *trans*-OMCA is mixed with CTAB, the counterions will strongly associate with CTAB micelles, causing micellar growth. Upon UV irradiation, *trans*-OMCA is converted to *cis*-OMCA, which has a much weaker interaction with CTAB, and will therefore tend to desorb from the micellar interface. As a result, the effective area of the CTAB headgroups increases, inducing the micelles to transform into much smaller structures and, thereby, driving the sharp drop in solution viscosity.

Last, it is worth discussing the generality of our results as well as the reversibility of the viscosity changes. We have observed similar light-induced viscosity transitions with several aromatic derivatives similar to OMCA, including cinnamic acid and *ortho*-coumaric acid. Thus, the results and mechanism presented here should extend to a range of aromatic derivatives. With regard to reversing the viscosity changes, we note from the UV-vis spectra that *trans*-OMCA has a much higher absorption than *cis*-OMCA over the entire wavelength range, which precludes a reverse *cis* to *trans* photoisomerization (but an acid-catalyzed reversal is possible²¹). Nevertheless, a variety of other organic molecules do permit reversible photoisomerizations,¹⁵ and the key will be to employ a molecule whose photoisomers have different effects on micellar self-assembly. Further work in this context is ongoing in our labs.

4. Conclusions

We have demonstrated light-responsive rheological properties in a class of micellar fluids consisting of the cationic surfactant, CTAB, and the organic derivative, OMCA. When OMCA is in

its *trans* form, it associates strongly with CTAB, leading to the formation of long, wormlike micelles. These micelles entangle into a transient network and thereby give rise to a highly viscoelastic fluid. Upon irradiation by UV light, *trans*-OMCA is photoisomerized to *cis*-OMCA. The *cis* isomer has a much weaker interaction with CTAB since its geometry does not favor binding at the micellar interface and also because it is more hydrophilic. Consequently, the *cis* isomer tends to desorb from the micellar interface, transforming the micelles into much smaller structures. As a result, the sample is converted into a low-viscosity, Newtonian fluid. A drop in zero-shear viscosity by several orders of magnitude can be induced in these fluids upon light irradiation for a few minutes. These photorheological (PR) fluids could thus be promising for use in microscale flow-control devices and sensors.

Acknowledgment. This work was funded by a seed grant from the Small Smart Systems Center (SSSC) at UMD and a CAREER award from NSF-CTS. Undergraduate students, Jamie Chandler and Joanna Tinnirella, helped with some of the rheology experiments. We are grateful to Angela Lewandowski and Professor Bill Bentley for help with the HPLC measurements. Finally, we would like to acknowledge NIST for facilitating the SANS experiments performed as part of this work.

Supporting Information Available: Details on sample characterization using HPLC are described in this section of the paper. This information is available free of charge via the Internet at <http://pubs.acs.org>.

JA065053G

(21) Noyce, D. S.; King, P. A.; Kirby, F. R.; Reed, W. L. *J. Am. Chem. Soc.* **1962**, *84*, 1632–1635.